Convective Boiling and Condensation Heat Transfer with a Twisted-Tape Insert for R12, R22, R152a, R134a, R290, R32/R134a, R32/R152a, R290/R134a, R134a/R600a

Mark A. KEDZIERSKI [†], Min Soo KIM [‡]

Abstract

Measured, local-average Nusselt numbers (Nu) for in-tube, convective boiling and condensation with a twisted-tape insert are presented for: R12, R22, R152a, R134a, R290, R32/R134a, R32/R152a, R290/R134a, and R134a/R600a. The heat transfer data were obtained from a fluid heated/fluid cooled, 9.7 m long condenser and evaporator of a breadboard refrigeration cycle. Convective-boiling, heat-transfer data were taken for transition and turbulent all-liquid Reynolds numbers. Convective-condensation, heat-transfer data were taken for laminar and turbulent all-liquid Reynolds numbers. The measured convective boiling and condensation Nusselt numbers for the single component and the azeotropic mixtures were each correlated to a single expression consisting of a product of dimensionless properties. The single component convective-boiling correlation was modified to predict the zeotropic mixture data. The predictions obtained from the modified flow-boiling correlations found in the literature were significantly different from the present Nusselt number measurements. Presumably, the correlations from the literature could account for neither the partial dryout induce by the tape nor the bubbly-mist flow introduced by an expansion valve.

KEYWORDS: *Enhanced heat transfer, refrigerant mixtures, flow boiling, in-tube condensation, twisted tapes, natural refrigerants*

Nomenclature

English symbols

a	constant in Eqs. 1 and 2 , K
A_c	cross-sectional flow area, m^2
b	constant in Eq. 2, K/m
Bo	local boiling number, $\frac{q''}{G\,h_{fg}}$
c	constant in Eqs. 1 and 2 , K/m^2
c_p	specific heat, J/kg·K
D_h	hydraulic diameter, m
D_i	inner diameter of tube, m
E_h	relative U (%) in h
f	Fanning friction factor
G	mass velocity of empty tube, $kg/m^2 \cdot s$
h	local-averaged heat-transfer coefficient, $W/m^2 \cdot K$
h_{fg}	latent heat of vaporization, kJ/kg
H	180° twist pitch, m
Ja	Jakob number, $c_{pf}\Delta T_s/h_{fg}$
k	liquid thermal conductivity, W/m·K
Nu	local-average Nusselt number based on D_i
$\dot{m}$	mass flow rate, kg/s
M	gram-molecular weight, g/mole
P	local fluid pressure, Pa
P_c	critical pressure, Pa
Pr	local liquid Prandtl number
q"	local heat flux, W/m^2
Re_D	all liquid, empty tube Reynolds number, $\frac{\rho_l G D_i}{\mu_l}$
Re_s	all liquid, swirl Reynolds number
Sw	swirl parameter
T	temperature, K
UA	overall conductance, W/K
U	expanded uncertainty for 95% confidence
V_a	mean axial velocity $\left(\frac{\dot{m}}{\rho_l A_c}\right)$, m/s
V_s	swirl velocity, m/s
x	mole fraction
x_q	thermodynamic mass quality
X	normalized axial heat exchanger coordinate
y	twist ratio, H/D_i

Greek symbols

α	exponent on correlation
δ_t	thickness of twisted tape, m
ΔL	heat transfer length of one increment, m
ΔT_s	wall superheat or wall subcooling, $\lvert T_w - T_s \rvert$, K
Δq	duty of one element, W
Θ	dimensionless mixture temperature difference, $(T_d - T_b)/(T_{LV} - T_{MV})$
μ	liquid dynamic viscosity, kg/m·s

* Received: October 30, 1997, Editor: Shoichiro FUKUSAKO, Susumu KOTAKE

† Building Fire and Research Laboratory, National Institute of Standards and Technology (Bldg. 226 Room B114, Gaithersburg, MD 20899, USA)

‡ Seoul National University, Seoul 151-742, Korea

X_{tt} Martinelli parameter

subscripts

a	annulus
b	bubble point
c	condensation
d	dew point
e	boiling
l	liquid, liquid composition
LV	less volatile component
m	mixture
MV	more volatile component
p	single component\azeotrope
r	parameter normalized by critical value
s	saturated state
t	twisted tape
v	vapor, vapor composition
w	inner tube wall
x	local-averaged quantity

1 Introduction

Twisted-tape inserts have been used to enhance heat transfer since the 19th century. Marine steam boilers were fitted with "retarders" (twisted tapes) to reduce coal consumption. Research began to appear in the literature around this time. In one of the first studies, Whitham [1] showed that twisted-tapes resulted in a 18.4% fuel savings for a coal-fired, horizontal, tube boiler of a Philadelphia railway station. In a more recent study, Marner and Bergles [2] reported 300% enhancements over the heat transfer of empty tubes for single phase flow with twisted-tape inserts. In the time between the Whitham (1896) [1] and the Marner and Bergles (1978) [2] publications, 90 manuscripts were published on the enhancement of single phase convection with swirl flow devices [3]. As of 1995, the number of publications on the subject had grown to 261. Over the years, the vibrant interest in the study of twisted tapes as a heat transfer augmentation has been sustained by its affordability and its suitability for retrofitting existing shell-and-tube heat exchangers.

The flow enhancement of the twisted tape arises primarily from increased flow path length and swirl mixing. Swirl flow and increased path length are expected to also benefit two-phase heat transfer. For example, Royal and Bergles [4] surveyed horizontal, convective condensation with twisted tapes and found improvements in heat-transfer coefficients by as much as 30% over empty tube condensation. In addition, the most popular use of twisted tapes in flow boiling is to delay the occurrence of burnout [5,6,7]. Yet, relatively few two-phase heat transfer studies with twisted tapes exist: approximately ten convective condensation and possibly 60 flow boiling. Furthermore, to the best of the authors' knowledge, no two-phase heat transfer studies with alternative refrigerants nor refrigerant mixtures for twisted tapes exist. This is unfortunate considering that using twisted tapes is an inexpensive way to reduce heat exchanger size or improve cycle efficiencies. Consequently, there is a need for phase change heat transfer data that can be used to design heat exchangers with twisted-tape inserts for alternative refrigerants and mixtures.

This paper presents measured local-averaged heat-transfer coefficients for in-tube convective boiling and condensation of several possible alternative refrigerants with a twisted-tape insert. The heat transfer performance of five single component and two azeotropic refrigerants were examined: R12, R22, R152a, R134a, R290, R290/R134a (0.44/0.56 % mass), and R134a/R600a (0.81/0.19 % mass). Also, the performance of two zeotropic refrigerant mixtures - R32/R134a, and R32/R152a - were examined at approximately five different mass compositions of R32 ranging from 15% to 40% R32. The heat transfer tests of the various working fluids were used in an attempt to develop universal-fluid evaporative and condensing heat transfer correlations.

Improved evaporator and condenser designs can be realized with the use of local heat transfer correlations. Local heat transfer correlations can be used to tailor evaporators and condensers for quality ranges and flow rates that are germane to a particular application. True local heat transfer measurements could have been obtained with an electrically heated test section. However, electric resistance heating is not a physically realistic boundary condition for refrigerant cycle applications. Accordingly, local-averaged heat-transfer coefficient measurements were obtained from a fluid heated test section that was divided into several segments. The heat-transfer coefficient was averaged over a particular range of qualities for each segment providing quasi-local (local-averaged) data. Kattan, et al. [8], Goto, et al. [9], and Conklin, et al. [10] provide examples of local-averaged flow-boiling experiments. An additional uncertainty in the heat-transfer coefficient is introduced by the averaging process. If the variation of the heat-transfer coefficient over the quality range for which it was averaged is sufficiently small, the uncertainty is negligible.

2 Test Apparatus

Figure 1 is a schematic of the breadboard refrigeration cycle from which the heat transfer measurements were made.

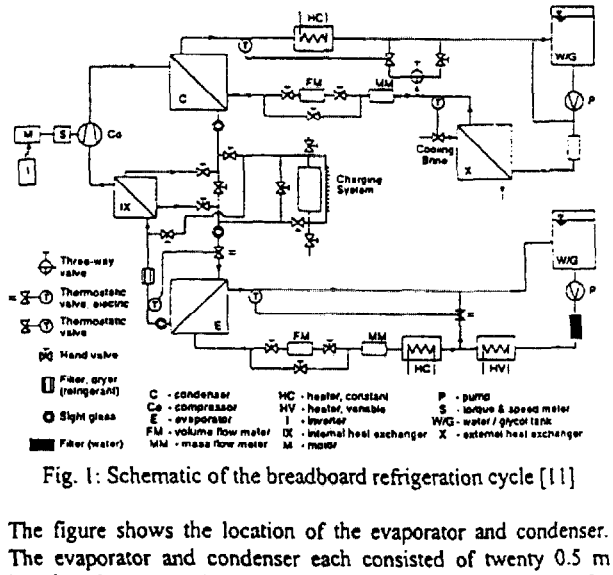

Fig. 1: Schematic of the breadboard refrigeration cycle [11]

The figure shows the location of the evaporator and condenser. The evaporator and condenser each consisted of twenty 0.5 m lengths of copper spined pipes with a snugly fitting copper tube over the spined fins. The twenty horizontal segments were stacked vertically and joined in series by u-bends and T-connections as shown in Fig. 2. The test refrigerant flowed through the 9.64 mm inner diameter tube which contained an aluminum twisted-tape insert. The 180° twist-pitch-to-tube-diameter ratio (twist ratio, y) was 4.15 and the tape thickness (δ) was 0.5 mm. A 40% mass glycol/water mixture flowed through the spined annulus counterflow to the refrigerant. The refrigerant was delivered to the

entrance of the evaporator by a thermostatic expansion valve at approximately 12% quality. Refrigerant vapor exited the evaporator with approximately 14 K of superheat. An open-drive, reciprocating compressor supplied superheated vapor to the condenser entrance. The refrigerant exited the condenser as subcooled liquid. Although neither an oil separator nor an accumulator were used in the cycle, the measured oil concentration was below the accuracy of our measurement which was 0.1%. Further details of the cycle can be found in Pannock and Didion [11].

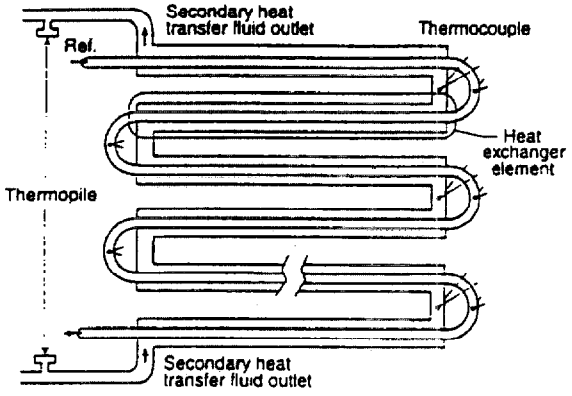

Fig. 2: Schematic of evaporator or condenser with thermocouple locations

Figure 2 illustrates the flow paths in the heat exchanger and the location of the refrigerant and the secondary fluid temperature measurements. The geometry and the size of the evaporator and condenser were practically identical. Thermocouples were epoxied to the outside of the refrigerant tube bends and insulated. Instream thermocouples were located in ever other bend of the secondary fluid stream. A ten-element, instream thermopile was used to measure the temperature change in the secondary heat transfer fluid across the entire heat exchanger.

Fluid mixers were not used before the thermopile ends. From past experience when mixers were used in other experiments, the expanded uncertainty (U) of the temperature difference measurement with thermopiles was estimated to be within 0.001 K to 0.01 K. (The expanded uncertainty estimates were obtained from a root-sum-square of the component uncertainties with a 95% confidence interval.) Two bends and 0.2 m of unheated/insulated length at the exit of the heat exchanger provided some mixing and time to approach a uniform temperature before the thermopile. The inlet fluid was mixed well. Considering that the mixed state of the heat transfer fluid at the heat exchanger exit was not as certain as the inlet, the expanded uncertainty (U) was estimated to be 0.1 K.

The conduction and mixing errors introduced by the indirect measurement of the refrigerant temperature at the insulated tube bend wall can be relatively small for a thin tube wall and small driving temperature differences. Errors in the refrigerant temperature measurement due to conduction of heat along the tube wall from the active portion of the heat exchanger to the insulated tube bend were modeled as one-dimensional heat conduction. The conduction error estimated using this method typically ranged (depending on the q") from $0.0009\Delta T_s$ ($=|T_w - T_s|$) to $0.009\Delta T_s$ or within 0.3 K for most heat fluxes. Mixing errors, those caused by a nonequilibrium refrigerant state at the point of temperature measurement, are due to insufficient mixing of the superheated sublayer in the adiabatic tube bend. Swirl and bend flow should contribute to some mixing of the refrigerant to an equilibrium state. However, a maximum mixing error can be estimated if it is assumed that no mixing occurs in the bend, and the problem is simplified to a transient conduction problem. Using this method the liquid sublayer was estimated to come within $0.08\Delta T_s$ of the saturation temperature by the time it reached the apex of the tube bend. Considering that ΔT_s varied on average from 1 K to 11 K for boiling and from 1 K to 6.5 K for condensation, the maximum error was estimated to be within 0.88 K and 0.52 K for boiling and condensation, respectively. Combining the conduction and mixing errors, the maximum error was estimated to be within 0.92 K. Considering that the swirl and bend flows contribute some mixing, the maximum refrigerant temperature measurement error should be less than 0.92 K.

The mass flow rates of the 40% mass glycol/water mixtures were measured with Coriolis flow meters having an expanded uncertainty of 0.001 kg/s. Turbine flow meters were used as a secondary flow rate measurement. The turbine meter measurements agreed with the measurements obtained from the Coriolis meters to within the uncertainty of the turbine meter. The refrigerant mass flow rate ($\dot{m}_r$) was calculated from an energy balance on the entire evaporator. The relative expanded uncertainty of $\dot{m}_r$ was 2% to 3%. The average thermodynamic quality (x_q) for each heat exchanger element was calculated from an energy balance on that element. The relative expanded uncertainty of x_q was within 7% of the measurement. Table 1 shows the estimated relative uncertainty, U (%), for various measurements.

Table 1:
Average Expanded Relative Measurement Uncertainties (%)

Parameter	U (%)
q_e	4
q_c	4
Re	3
P_r	.5
Bo	8
UA_s	7
ΔT_{lmx}	7
$\dot{m}_{Turbine}$	10
$\dot{m}_{Coriolis}$	3
h_s	17
$q_e"$	5
$q_c"$	8
Ja	3

3 Data Reduction Methodology

Figure 3 shows the refrigerant and secondary fluid temperature profiles for a R22 evaporator and condenser. The temperatures are plotted against a dimensionless coordinate (X) which represents a fraction of the axial length of the heat exchanger. For example, the refrigerant entrance to the evaporator and the condenser is shown at X = 0 and X = 1, respectively. At approximately X = 0.88, saturated refrigerant vapor exists for both the evaporator and the condenser. The vapor is superheated for values of X greater than approximately 0.88. Heat-transfer data reported here are only for the two-phase region, i.e., for thermodynamic qualities between 0 and 1.

The uncertainty in the Nusselt number was reduced by using a regression of the secondary fluid temperatures to X in its calculation. Figure 3 shows that the scatter in the evaporator secondary fluid temperature profile is marginally greater than that exhibited in the condenser secondary fluid temperature. A weighted regression was used to reduce the uncertainty caused by random effects in secondary temperature measurement. Those

evaporator secondary fluid temperatures (T_f) not associated with the superheated refrigerant vapor were fitted to:

$$T_f = a + cX^2 \quad (1)$$

The weighted regression takes advantage of the stability of the inlet secondary fluid temperature measurement. Unfortunately, the

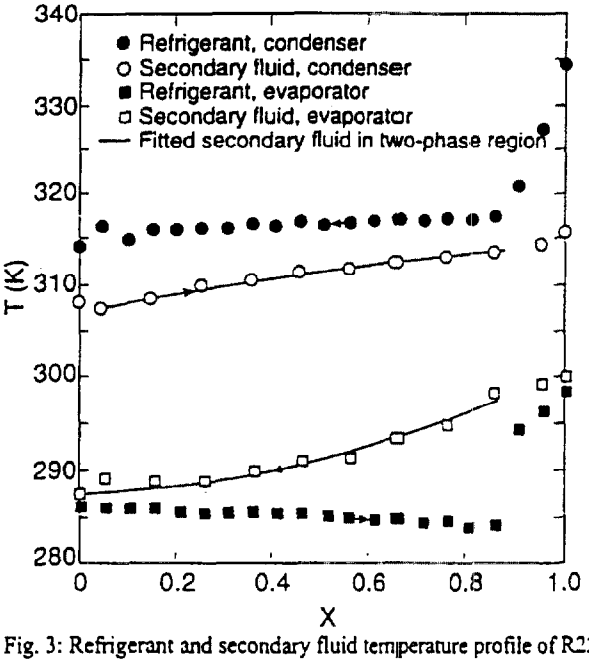

Fig. 3: Refrigerant and secondary fluid temperature profile of R22 evaporator and condenser

inlet secondary fluid temperature was omitted from the fit because it lies in the superheated refrigerant region. To overcome this, the exit secondary fluid temperature was calculated from the inlet temperature and the temperature change obtained from the thermopile. The variance of the calculated exit fluid temperature was approximately 25 times smaller than that of the secondary fluid temperature measurements taken in the heat exchanger bends. Accordingly, a weighing factor of 25 was used on the exit fluid temperature. Only a 0.3% change in the model coefficients occurred when the weighing factor was decreased from 25 to 15. Consequently, a negligible error is introduced for a large error in the estimate of the weighing factor.

A weighing factor was not used for the condenser calculation because of the relatively small scatter of the secondary fluid temperature measurements and because the exit and inlet secondary fluid temperatures were not associated with two-phase refrigerant flow. Nevertheless, the secondary fluid temperatures were fitted to X to reduce the uncertainty in the measurement. As shown in Fig. 3, the form of the condenser secondary fluid temperature differs from that of the evaporator. Consequently, the secondary fluid temperatures associated with the two-phase refrigerant of the condenser were fitted to:

$$T_f = a + bX + cX^2 \quad (2)$$

The forms of Eqs. 1 and 2 provided the best fit of the measurements with the minimum number of terms.

The overall conductance (UA) equation can be written for a single 0.5 m long heat exchanger element as:

$$\frac{1}{UA} = \frac{\Delta T_{lm_x}}{\Delta q} = \frac{1}{h_t A_t} + \frac{\ln\left(\frac{D_r}{D_i}\right)}{2\pi\Delta L k_{cu}} + \frac{1}{\eta h_a A_o} \quad (3)$$

The h_t is the heat-transfer coefficient of the inner smooth tube with the twisted-tape insert and is based on the empty tube-side area A_t ($\pi D_i \Delta L$.) The next to the last term is the thermal resistance of the tube wall between the fluids. The h_a represents the heat-transfer coefficient for the spine-fin annulus. Kedzierski and Kim [12] developed a single phase heat transfer correlation for a spine-fin annulus with the same geometry as the spine-fin annulus in the present test heat exchangers. It was presumed that the bends destroyed the fully developed thermal boundary layer. Consequently, the h_a correlation was used to account for thermally developing flow in each element.

The log-mean temperature difference (ΔT_{lmx}) was calculated for each increment using the measured refrigerant temperatures and the secondary fluid temperatures from Eqs 1 and 2. The effective heat capacity of a zeotropic mixture is nearly constant for each increment. Consequently, the error introduced in using the log-mean temperature difference equation was negligible.

The duty for the ith element was calculated from Eq. 2 as:

$$\Delta q = \dot{m}_r \, c_{p_r} \left(b(X_{i+1} - X_i) + c(X_{i+1}^2 - X_i^2) \right) \quad (4)$$

where X_i and X_{i+1} are evaluated at the refrigerant inlet and exit of each increment of length ΔL, and b is zero for the evaporator. All of the core elements were 0.5 m in length. The length of the end elements were shortened in an appropriate amount to account for the single phase heat transfer in the element.

The local-average heat-transfer coefficient (h_t) was calculated from Eq. 3 as:

$$h_t = \left(\frac{A_t \Delta T_{lm_x}}{\Delta q} - \frac{A_t \ln\left(\frac{D_r}{D_i}\right)}{2\pi\Delta L k_{cu}} - \frac{A_t}{\eta h_a A_o} \right)^{-1} \quad (5)$$

The average expanded uncertainty for the h_t was within 9% for all of the data.

4 Test Results

Over 200 graphs would be required to plot the measured local-averaged heat-transfer coefficient (h_t) versus thermodynamic quality for each test run. Instead, only representatives plots of h_t are presented in Fig's 4 and 5 for R22 flow boiling and R134a convective condensation, respectively. Tables containing all of the measured data generated in this study and h_t versus quality plots for all of the fluids are presented by Kedzierski and Kim [13]. Several different predictive correlations are compared to the measured data in the h_t plots. A more detailed discussion of the predictions and the measurements follows.

4.1 Convective Condensation

Figure 4 shows the measured local-averaged, convective-

condensation, heat-transfer coefficient (h_t) as a function of thermodynamic quality for R134a. The data are compared to predictions from four different correlations. No universal-fluid local convective-condensation coefficients for twisted tapes were found in the literature. Three universal-fluid, smooth-tube, horizontal, convective-condensation correlations were modified according to a procedure given by Royal and Bergles [14]. The procedure, as explained below, permits the smooth-tube condensation correlations of Soliman [15], Shah [16], and Traviss et al. [17] to account for the enhancement of the twisted tape. The fourth correlation, shown as a solid line, is a fit of the measurements. No general convective condensation correlations for azeotropic/zeotropic mixtures were found in the literature. Consequently, the mixture properties were used in the pure component condensation correlations to predict the mixture heat transfer.

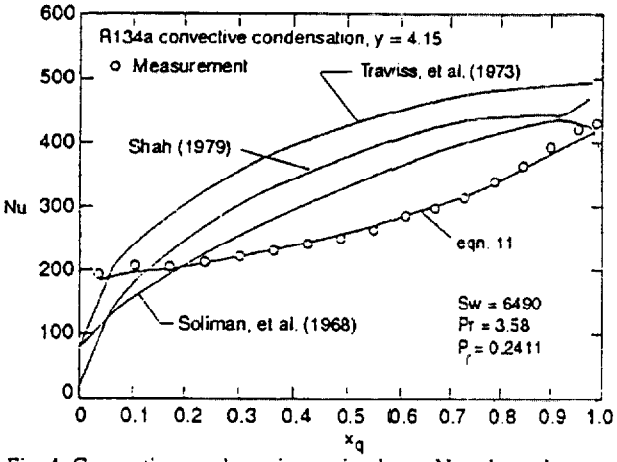

Fig. 4: Convective condensation, twisted-tape Nusselt number as a function of thermodynamic quality for R134a

Royal and Bergles [14] suggested that the twisted-tape Reynolds number (Re_s) replace the smooth tube Reynolds number and that a fin-effect correction be used. The fin-effect correction was not used because later work by Manglik and Bergles [18] proved it to be negligible for snug to loose fitting tape inserts. The swirl Reynolds number (Re_s) is based on the swirl velocity (V_s) and the hydraulic diameter of the tube with the twisted-tape insert:

$$Re_s = \frac{\rho_l V_s D_h}{\mu_l} = Re_D \frac{\sqrt{1 + \left(\frac{\pi}{2y}\right)^2}}{1 - \frac{4\delta}{\pi D_i}} \qquad (6)$$

The adjustment to Re_D in Eq. 6 is $\frac{V_s D_h}{D_i V_a}$ where V_a is the mean axial velocity of the liquid.

For most of the data, the measured condensation heat-transfer coefficient decreases for decreasing qualities. Apparently, thin liquid films and high vapor velocities at the entrance of the condenser provide for high heat-transfer coefficients. As the liquid accumulates on the tube wall for decreasing quality, the heat-transfer coefficient diminishes. The decrease in the heat-transfer coefficient from a quality of 0.4 to that of 0.05 is relatively modest compared to the decrease shown by the predictive correlations available in the literature. For example, all of the predictions by correlations from the literature show at least a factor of two increase in h_t for qualities from 0.05 to 0.4. Presumably, the modification to the smooth tube correlation does not completely account for the swirl enhancement for the lower qualities.

Several generalizations can be made, for all of the fluids, concerning the ability of the available correlations to predict the measured heat transfer data. For example, the Soliman [15], the Shah [16], and the Traviss et al. [17] correlations were nearly always parallel, intersecting only at high and low qualities. Typically these correlations were within 15% to 25% of one another. The Soliman [15] correlation more closely predicted the measured Nusselt Numbers than the Shah [16], and the Traviss et al. [17] correlations did. The Traviss et al. [17] correlation consistently gave the largest overpredictions for x_q greater than 0.4. As a group, the correlations typically overpredict the measured Nusselt numbers from 10% to 100% for qualities greater than 0.4 with the greatest overpredictions occurring for the higher qualities.

4.2 Flow Boiling

Figure 5 shows the measured, local-averaged, flow-boiling, heat-transfer coefficient (h_t) as a function of thermodynamic quality.

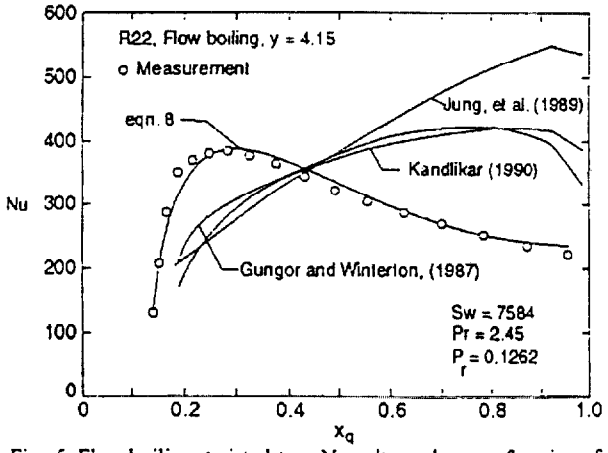

Fig. 5: Flow boiling, twisted-tape Nusselt number as a function of thermodynamic quality

The data are compared to predictions from three different modified smooth tube correlations. The smooth tube flow-boiling correlations of Jung et al. [19], Kandlikar [20], and Gungor and Winterton [21] were modified in the same manner as the condensation correlations were modified to account for the effect of the twisted tape. Namely, the Re_D was replaced with Re_s wherever it was encountered in the smooth tube correlations. The Jung et al. [19] correlation was the only one valid for both pure components and mixtures. The pure component correlations of Kandlikar [20], and Gungor and Winterton [21] were used with mixture properties to predict the mixture heat transfer. A reasonable fluid factor that gave a favorable comparison to the data was used in the Kandlikar [20] correlation for the mixture predictions.

The shape of the measured h_t versus x_q plots is similar for the various fluids. For each fluid, the measured h_t exhibits two distinct regions intersecting at approximately $x_q = 0.35$. The bubbly flow region and the convective flow region reside for approximately x_q

< 0.35 and for $x_q > 0.35$, respectively. The data exhibits a small negative slope in the convective region. In the bubbly flow region, relatively large increases in the heat-transfer coefficient occur for small increases in the quality. Speculation on the basis of the relationship between h_t and x_q in the convective and bubbly flow regions is presented in the following four paragraphs.

The decrease in the measured h_t in the convective region can be attributed to increasing partial dryout of the tube wall with increasing quality. The twisted tape encourages dryout with a 64% greater surface perimeter than that of an empty tube. Consequently, liquid that would have wetted the wall of the empty tube is drawn/impelled to the tape by surface-tension and vapor acceleration forces. Dry areas on the tube wall become more prevalent as less liquid is available to wet the wall and larger heat fluxes are available to evaporate the thin liquid films.

The promotion of partial dryout by a twisted tape does not contradict the notion that twisted tapes can be used to delay burnout. Bergles et al. [6] conjecture that the critical heat flux condition in dispersed flow is delayed as a result of centrifugal flow forces which impel small liquid droplets to the outer wall for evaporation. As noted by Bergles et al. [6], droplet impinging does not nullify tape wetting even in dispersed flow. Consequently, the twisted tape can simultaneously benefit and deter heat transfer at high qualities by delaying burnout and inducing partial dryout, respectively.

The correlations from the literature depict a trend that is contrary to that of the measured data. The correlations taken from the literature predict an increasing heat-transfer coefficient with quality for nearly the entire quality range. To the best of the authors' knowledge, all the literature correlations were developed with data primarily from electrical resistance heated test sections. It is unlikely that any partial dryout data was included in these correlating data sets. Tube dryout for an electrically heated test section would present a destructive burnout condition. Consequently, the literature correlations present a case where the walls remain wetted as the quality increases. For this case, increasing vapor shear and decreasing film thickness with increasing quality act to enhance the heat transfer.

Figure 6, a sample plot of the heat flux versus wall superheat (ΔT_s), aids in explaining the h_t versus quality trend in the bubbly flow region. As seen in Fig. 6, the heat flux is relatively small but rapidly increasing in the low-quality region. Accordingly, little change in the quality occurs in the bubbly flow region because the energy input is small. The h_t follows the rapidly increasing heat flux because the wall superheat is nearly constant in this region. The rapid increase in the heat flux is a consequence of the counterflow heat exchange between the refrigerant and the secondary fluid. The constant superheat results from the boiling flow pattern. For example, little, if any, bubble nucleation occurs in the bubbly flow region because of the small heat flux. Instead, tiny bubbles originate from the expansion valve. For example, Aaron and Domanski [22] describe the flow after an expansion device as a misty jet. The ΔT_s remains relatively small and constant in the bubbly flow region because: (1) the vapor is thoroughly interspersed within the liquid resulting in a near equilibrium state, and (2) a negligible amount of superheat is required to maintain and grow established bubbles. Liquid superheat occurs for qualities greater than 0.35 because the vapor has coalesced and segregated itself from the liquid. In summary, the rapidly increasing h_t in the low-quality region results from a rapidly increasing heat flux while the refrigerant liquid at the wall remains near saturation. Consequently, the authors anticipate that their boiling correlation would be valid in the low-quality range for refrigeration cycles where bubble mist flow is introduced in the evaporator in the absence of bubble nucleation at the wall.

Considering the different conditions for which the present data was taken and the literature correlations were derived, it is not surprising that the predictions and the measurements differ. The predicted pure fluid Nusselt numbers obtained from the modified correlations of Jung et al. [19], Kandlikar [20], and Gungor and Winterton [21] were relatively consistent with one another. For the most part, these correlations over-predict the measured Nusselt numbers for convective region and under-predict those for the bubbly flow region. It was not uncommon for the convective region to be over-predicted by 100%. The Nusselt numbers obtained from the modified correlations typically predicted the measured Nusselt numbers for the bubbly flow region to within 50%. In contrast to predictions for the pure fluids, the azeotropic predictions from the Kandlikar [20] correlation were as much as 30% lower than those obtained from the Jung et al. [19], and the Gungor and Winterton [21] correlations which remained consistent

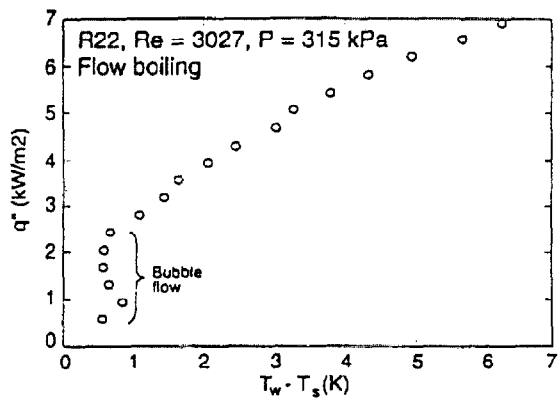

Fig. 6: Sample plot of the heat flux vs. wall superheat with each other.

5 Correlations

From the previous section it is obvious that the modified existing correlations do not reliably predict the present data. The following section presents three correlations that were derived from the present Nusselt number measurements. The three correlations quantify the local Nusselt numbers for convective boiling and condensation of pure/azeotropic and zeotropic fluids within a tube with a twisted-tape insert. The fluid properties and heat transfer conditions used in the correlations were evaluated locally.

Manglik and Bergles [23] suggest that swirl flow effects may be correlated by the swirl parameter (Sw):

$$Sw = \frac{Re_s}{\sqrt{y}} \tag{7}$$

The $1/\sqrt{y}$ parameter accounts for convective inertia effects that are ignored by $1/y$ which has been traditionally used to correlate swirl flow data. Manglik and Bergles [23] show that laminar flow heat transfer for three different twist ratios are correlated well with the swirl parameter. Agrawal et al. [24] also correlated R12 swirl flow-boiling heat-transfer coefficients to $y^{-0.5219}$ for Re_D approximately in the range of 7000 to 14000.

Consequently, it is inferred that the $1/\sqrt{y}$ parameter is suitable for correlating flow boiling and convective condensation data for low and somewhat high Reynolds numbers.

The Law of Corresponding States philosophy presented by Cooper [25] was followed by including the reduced pressure (P_r), the acentric factor ($-\log_{10}P_r$) and the molecular weight (M) in the correlation. Cooper [25] suggests that the fluid properties that govern nucleate pool boiling can be well represented by a product of these variables to various powers. The above terms and several others were used to correlate our data for all conditions of two-phase flow.

The Nusselt number correlations were derived from phase change data taken in a 9.6 mm diameter tube with a twisted-tape of twist ratio 4.15, and for $1000 < Sw < 180000$, $2.8 \times 10^{-5} < Bo < 5.1 \times 10^{-4}$, $0.007 < Ja < 0.1$, and $0.032 < P_r < 0.34$. More detail for the ranges of these and other parameters is given in Kedzierski and Kim [13]. The heat transfer measurements were fitted to three separate correlations. The convective condensation Nusselt numbers for single component, azeotropic, and zeotropic fluids were fitted to a single equation. Two equations were necessary to correlate the flow boiling Nusselt numbers of refrigerants and refrigerant mixtures. The data were fitted to fundamental dimensionless parameters in hopes that the correlations could be extrapolated to other fluids, tube diameters, and twist ratios. There is no way to know a priori how well the equations will perform when they are extrapolated beyond the conditions of the data base.

There are several details that are common to all three of local Nusselt number correlations that follow. First, all of the parameters were evaluated locally. Each parameter is raised to a nonconstant exponent which is a quadratic function of quality. The quality dependent exponents enable the single correlation to predict most of the two-phase region. For example, as will be seen in Eq 8, the exponent on the boiling number (Bo) is relatively large in the low quality region and decreases for the high quality region. Finally, all Nusselt number measurements with a relative expanded uncertainty greater than 12.5% where omitted from the regression. The omissions resulted in a loss of approximately 1% of the data.

The boiling data was taken for transition and turbulent all-liquid Reynolds numbers (Re_D). The condensation data were taken for laminar and turbulent all-liquid Reynolds numbers. The all-liquid Reynolds were evaluating using the local liquid properties of the fluid.

5.1 Flow-boiling

The 1401 locally measured flow-boiling Nusselt numbers for refrigerants R12, R22, R152a, R134a, R290, R290/R134a, and R134a/R600a were correlated to the following equation:

$$Nu_p = 1.356 \cdot Sw^{\alpha_1} \cdot Pr^{\alpha_2} \cdot P_r^{\alpha_3} \cdot (-\log_{10} P_r)^{\alpha_4} \cdot Bo^{\alpha_5} \quad (8)$$

where:

$$\alpha_1 = 0.993 - 1.181x_q + 0.899x_q^2$$
$$\alpha_2 = 1.108 - 2.366x_q + 1.451x_q^2$$
$$\alpha_3 = -2.383 + 5.255x_q - 1.791x_q^2$$
$$\alpha_4 = -3.195 + 6.668x_q$$
$$\alpha_5 = 1.073 - 2.679x_q + 1.443x_q^2$$

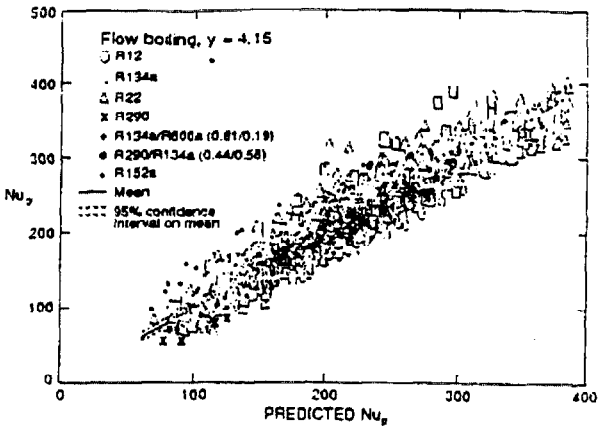

Fig. 7: Correlation of twisted-tape flow boiling of single components and azeotropic mixture Nusselt numbers

Figure 7 shows that Eq 8 correlates 95% of the pure component and azeotropic flow-boiling Nusselt numbers to within approximately ± 25%. The mean of the measurements has an expanded uncertainty of ± 5%. Only random trends were observed in the residual plots

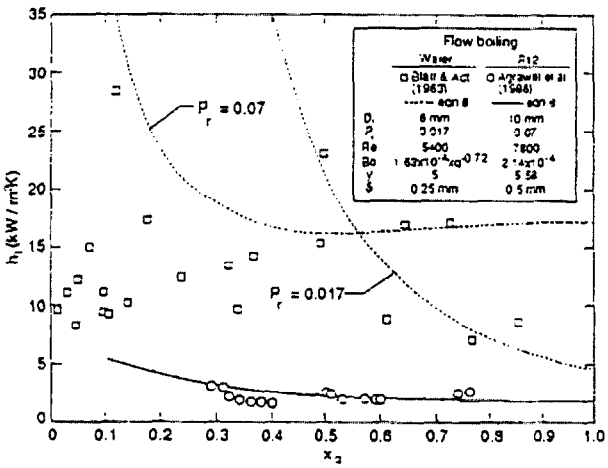

Fig. 8: Comparison of twisted-tape flow boiling correlation of data available in the literature

against each of the parameters of Eq. 8. Equation 8 is plotted as a solid line on figure 5.

Figure 8 compares Eq. 8 to measured flow-boiling heat-transfer coefficients from the literature. Agrawal et al. [24] present local R12 flow-boiling heat-transfer coefficients for a tube with a twisted tape with a twist ratio of 5.58. Equation 8 predicts the Agrawal et al. (1986) data to within 15% for qualities between 30% and 40%. Larger differences between Equation 8 and the Agrawal et al. [24] data were evident for higher heat flux conditions. Figure 8 also compares the locally measured water flow-boiling heat-transfer coefficients by Blatt and Adt [26] to Eq. 8 for a twist ratio of 5. A precise assessment of Eq. 8 using the Blatt and Adt [26] data is difficult due to the large scatter in the data. Also, Blatt and Adt [26] did not give the test pressure in their manuscript. As a result, Eq. 8 is plotted using two likely test pressures. The most that can be said is that the correlation passes through some of the data.

Schluender [27] developed a nucleate pool boiling model for binary zeotropic mixtures. His model includes the effects of Bo, the difference in the vapor and liquid mole fraction of the more volatile component (x_v - x_l), and the difference in the saturation temperature of the two pure components (T_{LV} - T_{MV}). Thome [28] criticizes the use of T_{LV} - T_{MV} and states that the mixture's boiling range would be a more appropriate parameter for the model. Accordingly, the present correlations contain the mole fraction difference, the Boiling number, and a dimensionless mixture temperature difference (Θ):

$$\Theta = \frac{T_d - T_b}{T_{LV} - T_{MV}} \tag{9}$$

where T_b and T_d are the local bubble point and dew point temperatures of the mixture, respectively.

The 935 zeotropic flow-boiling Nusselt numbers for R32/R152a and R32/R134a were fitted to:

$$\frac{Nu_m}{Nu_p} = 2.525 \cdot (x_v - x_l)^{\alpha_1} \cdot \Theta^{\alpha_2} \cdot P_r^{\alpha_3} \cdot Bo^{\alpha_4} \cdot M^{\alpha_5} \tag{10}$$

where:

$$\alpha_1 = -0.58 + 5.67x_q - 2.825x_q^2$$
$$\alpha_2 = -2.793x_q$$
$$\alpha_3 = 1.204 - 3.335x_q + 1.946x_q^2$$
$$\alpha_4 = 0.338 + 0.353x_q$$
$$\alpha_5 = 0.839$$

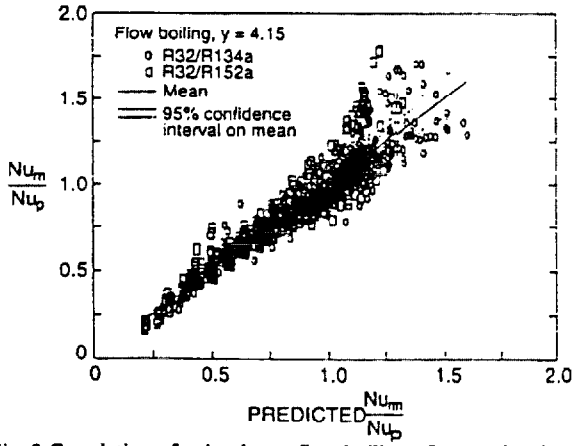

Fig. 9 Correlation of twisted-tape flow boiling of zeotropic mixture Nusselt numbers

where Nu_p was evaluated using Eq. 8 and the local properties of the zeotropic mixture.

Figure 9 shows that Eq 10 correlates 95% of the zeotropic flow-boiling Nusselt numbers to within approximately ± 20%. The mean of the measurements has an expanded uncertainty of ± 4%.. Only random trends were observed in the residual plots against each of the parameters of Eq 10.

5.2 Convective condensation

The 2253 locally measured convective condensation Nusselt numbers for refrigerants R12, R22, R152a, R134a, R290, R290/R134a, R134a/R600a, R32/R134a, and R32/R152a were correlated to the following equation:

$$Nu = 0.00136 \cdot Sw^{\alpha_1} \cdot P_r^{\alpha_2} \cdot Pr^{\alpha_3} \cdot (-\log_{10} Pr)^{\alpha_4} \cdot Ja^{\alpha_5} \tag{11}$$

where:

$$\alpha_1 = 0.613 + 0.647x_q$$
$$\alpha_2 = 0.877$$
$$\alpha_3 = -1.735 + 2.362x_q$$
$$\alpha_4 = -2.815 + 4.197x_q$$
$$\alpha_5 = -0.528$$

Figure 10 shows that Eq 11 correlates 95% of all the condensation Nusselt numbers to within approximately ± 20%. The single equation was found to acceptably predict single component and zeotropic Nusselt numbers equally well. This suggests that mass transfer has a negligible effect on condensation heat transfer with twisted tape-inserts. The mean of the measurements has an expanded uncertainty of ± 3%.

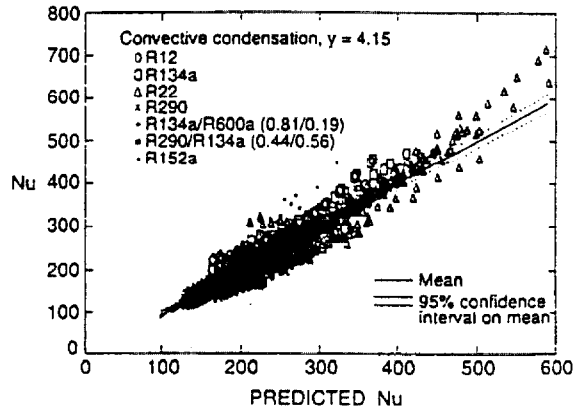

Fig. 10: Correlation of twisted-tape, convective condensation of single component and azeoptropic mixture Nusselt numbers

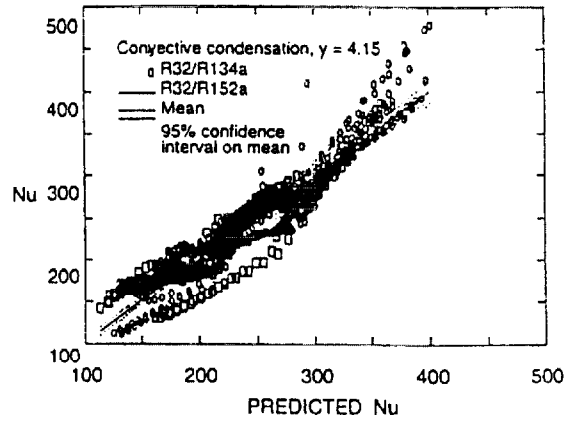

Fig. 11: Correlation of twisted-tape, convective condensation zeotropic mixture Nusselt numbers

Only random trends were observed in the residual plots against each of the parameters of Eq 11. Equation 11 is plotted as a solid line in figure 4.

6 Conclusions

The Nusselt numbers for flow boiling and convective condensation with a twisted-tape insert were measured and correlated for several single component, azeotropic, and zeotropic refrigerants. Three different correlations were developed to predict the flow boiling and convective condensation conditions for azeotropic and zeotropic refrigerants. The Nusselt numbers were correlated with dimensionless variables raised to nonconstant exponents. The nonconstant exponents enabled each single correlation to capture the variation of the relative importance of each parameter with quality. The flow-boiling correlations are valid for transition and turbulent all-liquid Reynolds numbers. The convective condensation correlation is valid for laminar and turbulent all-liquid Reynolds numbers, and for pure, azeotropic and zeotropic refrigerants.

The condensation measurements were compared to several smooth tube correlations that were modified to account for the effect of swirl flow. For the low quality region, the rate of decrease in the twisted-tape condensation-Nusselt number was significantly less than that predicted with the modified correlations. Also, the magnitude of the measured condensation-Nusselt numbers were significantly greater than the predictions for the low quality region. Presumably, the modification to the smooth tube correlation does not completely account for the swirl enhancement for the lower qualities.

The flow-boiling measurements were also compared to several smooth tube correlations that were modified to account for the effect of swirl flow. For the most part, the modified correlations significantly over predicted the measured boiling-Nusselt numbers in the convective region. It was conjectured that the twisted tape encouraged partial dryout of the tube wall. The partial dryout caused the Nusselt number to decrease with increasing quality. The modified correlations predicted an opposite trend with quality. Possibly, the fact that the modified correlations were derived from data obtained from electrical resistance heated rigs prohibits the prediction of the dryout effect. Also, the very low quality heat transfer measurements were not predicted very well by the modified correlations. An expansion valve supplied a bubbly-mist flow to the entrance of the evaporator. Consequently, no nucleation of bubbles occurred at the wall. This is in contrast to electrically heated test rigs where high superheats and bubble nucleation at low quality are common.

7 Acknowledgments

This work was jointly funded by NIST and the U.S. Department of Energy (project no. DE-AI01-91CE23808) under Project Manager Bill Noel. The authors thank the following NIST personnel for their constructive criticism of the first draft of the manuscript: Dr. D. Olson, Mr. J. Gebbie, and Mrs. J. Land. The authors express their appreciation to Dr. J. Pannock and Dr. M. H. Kim for their contributions towards data collection and test rig construction.

References

[1] Whitham, J. M., 1896, "The Effect of Retarders in Fire Tubes of Steam Boilers," Street Railway Journal, Vol. 12, No. 6, p. 374.

[2] Marner, W. J., and Bergles, A. E., 1978, "Augmentation of Tubeside Laminar Flow Heat Transfer by Means of Twisted-Tape Inserts, Static Mixer Inserts and Internally Finned Tubes," Heat Transfer 1978, Proceedings of the Sixth International Heat Transfer Conference, Hemisphere, Vol. 2, pp. 583-588.

[3] Bergles, A. E., Jensen, M. K., and Shome, B., 1995, "Bibliography on Enhancement of Convective Heat and Mass Transfer," HTL-23, Rensselaer Polytechnic Institute, Troy, NY.

[4] Royal, J. H., and Bergles, A. E., 1976, "Experimental Study of the Augmentation of Horizontal In-Tube Condensation," ASHRAE Trans., Vol. 82, Pt. 2, pp. 919-931.

[5] Gambill, W. R., Bundy, R. D., and Wansbrough, R. W., 1961, "Heat Transfer, Burnout, and Pressure Drop for Water in Swirl Flow Through Tubes with Internal Twisted Tapes," Chemical Engineering Progress Symposium Series, Vol. 57, No. 32, pp. 127-137.

[6] Bergles, A. E., Fuller, W. D., and Hynek, S. J., 1971, "Dispersed Flow Film Boiling of Nitrogen with Swirl Flow," Int. J. Heat Mass Transfer, Vol. 14, pp. 1343-1354.

[7] Papadopoulos, P., France, D. M., Minkowycz, W. J., Harty, J., Hamoudeh, M. N., and Wu, M.-S., 1994, "Two-Phase Dispersed Flow Heat Transfer Augmented by Twisted Tapes," Enhanced Heat Transfer, Vol. 1, No. 4, pp. 305-314.

[8] Kattan, N., Favret, D., and Thome, J. R., 1995, "R-502 and Two Near-Azeotropic Alternatives: Part I -- In-Tube Flow-Boiling Tests," ASHRAE Trans, Vol. 101, Pt. 1, pp. 491-508.

[9] Goto, M., Inoue, N., and Koyama, K., 1995, "Evaporation Heat Transfer of HCFC-22 and Its Alternative Refrigerants Inside an Internally Grooved Horizontal Tube," Proceedings of the 19th International Congress of Refrigeration, Vol. IVa, pp. 246-253.

[10] Conklin, J. and Vineyard, E., 1992, "Flow Boiling Enhancement of R-22 and a Nonazeotropic Mixture of R-143a and R-124 Using Perforated Foils," ASHRAE Trans, Vol. 98, Pt. 2, pp. 402-410.

[11] Pannock, J., and Didion, D. A., 1991, "The Performance of Chlorine-Free Binary Zeotropic Refrigerant Mixtures in a Heat Pump," NISTIR 4748, U.S. Department of Commerce, Washington.

[12] Kedzierski, M. A., and Kim. M. S., 1996, "Single-Phase Heat Transfer and Pressure Drop Characteristics of an Integral-Spine Fin Within an Annulus," J. of Enhanced Heat Transfer, Vol. 3, No. 3, pp. 201-210.

[13] Kedzierski, M. A., and Kim. M. S., 1997, "Convective Boiling and Condensation Heat Transfer with a Twisted-Tape Insert for R12, R22, R152a, R134a, R290, R32/R134a, R32/R152a, R290/R134a, R134a/R600a," NISTIR 5905, U.S. Department of Commerce, Washington.

[14] Royal, J. H., and Bergles, A. E., 1978, "Augmentation of Horizontal In-Tube Condensation by Means of Twisted-Tape Inserts and Internally Finned Tubes," J. of Heat Transfer, Vol. 100, pp. 17-24.

[15] Soliman, M., Schuster, J. R., and Berenson, P. J., 1968, "A General Heat Transfer Correlation for Annular Flow Condensation, J. Heat Transfer, Trans. ASME, Vol. 90, No. 2.

[16] Shah, M. M., 1979, "A General Correlation for Heat Transfer During Film Condensation Inside Pipes," Int. J. Heat Mass Transfer, Vol. 22, pp. 547-556.

[17] Traviss, D. P., Rohsenow, W. M., and Baron, A. B., 1973, "Forced-Convection Condensation Inside Tubes: A Heat Transfer Equation for Condenser Design," ASHRAE Trans.,

Vol. 79, Pt. 1, 157-165.

[18] Manglik, R. A., and Bergles, A. E., 1987, "A Correlation for Laminar Flow Enhanced Heat Transfer in Uniform Wall Temperature Circular Tubes with Twisted-Tape Inserts," Advances in Enhanced Heat Transfer - 1987, HTD Vol. 68, ASME, New York, pp. 19-25.

[19] Jung, D. S., McLinden, M. O., Radermacher, R., and Didion, D. A., 1989, "A Study of Flow Boiling Heat Transfer with Refrigerant Mixtures," Int. J. Heat Mass Transfer, Vol. 32, pp. 1751-1764.

[20] Kandlikar, S. G., 1990, "A General Correlation for Saturated Two-Phase Flow Boiling Heat Transfer Inside Horizontal and Vertical Tubes," J. Heat Transfer, Vol. 112, pp. 219-228.

[21] Gungor, and Winterton, 1987, "Simplified General Correlation for Saturated Flow Boiling and Comparisons of Correlations with Data," The Canadiam J. of Chem. Eng., Vol. 65, no. 1, pp. 148-156.

[22] Aaron, D. A., and Domanski, P. A., 1989, "An Experimental Investigation and Modeling of the Flow Rate of Refrigerant-22 Through the Short Tube Restrictor," NISTIR 89-4120, U.S. Department of Commerce, Washington, D.C.

[23] Manglik, R. A., and Bergles, A. E., 1992, "Heat Transfer and Pressure Drop Correlations for Twisted-Tape Inserts in Isothermal Tubes: Part I - Laminar Flows," Enhanced Heat Transfer, ASME, HTD-Vol. 202, pp. 89-98.

[24] Agrawal, K. N., Varma, H. K., and Lal, S., 1986, "Heat Transfer During Forced Convection Boiling of R12 Under Swirl Flow," J. Heat Transfer, Vol. 108, 1986 pp. 567-573.

[25] Cooper, M.G., 1984, Saturation Nucleate Pool Boiling- A Simple Correlation Vol. 86, Department of Engineering Science, Oxford University, England, pp 785-793.

[26] Blatt, T. A., and Adt, R. R., Jr., 1963, "The Effects of Twisted Tape Swirl Generators on the Heat Transfer Rate and Pressure Drop of Boiling Freon 11 and Water," ASME, paper # 63-WA-42.

[27] Schluender, E. U., 1982, "Uber den Warmeubergang bei der Blasenverdampfung von Gemischen, Verfahrens-Technik, Vol. 16, pp. 692-698.

[28] Thome, J. R., 1989, "Prediction of the Mixture Effect on Boiling in Vertical Thermosyphon Reboilers," Heat Transfer Engineering, Vol. 10, no. 2, pp. 29-38.